Mapping the Nucleotide-Dependent Conformational Change of Human N-ras p21 in Solution by Heteronuclear-Edited Proton-Observed NMR Methods†

Jin-Shan Hu and Alfred G. Redfield*

Department of Biochemistry, Brandeis University, Waltham, Massachusetts 02254

Received February 15, 1993; Revised Manuscript Received April 7, 1993

ABSTRACT: Heteronuclear-edited proton-detected NMR methods are used to study the nucleotide-dependent conformational change between GDP- and GTPγS-bound forms of human N-ras p21. Amide groups of Asp are used as sensitive probes. When GTPγS is substituted for GDP in cellular N-ras p21, the chemical shifts of resonances Asp-47, -126, -154, and Asn-172, as well as Gly-77 and -151, are not sensitive to nucleotide exchange, whereas Asp-30, -33, -38, -54, -57, -69, -92, -105, and -119 are affected. Distinct chemical shift changes of Asp-33, -38, and -69 indicate that substantial structural changes occur in the effector-binding region and the switch II region. Crystallographic studies of H-ras p21 have indicated that the conformational differences are confined to residues 32–38 and 60–76. Our observations indicate that the nucleotide-dependent structural transitions of the protein in solution may not be identical to those in the crystal. They suggest that the peptide beyond Glu-76 participates in a conformational switch, and possibly is involved in effector function. We propose that the region roughly from Asp-92 to -105, and the region of guanine base-binding motif(s), e.g., ^{116}NKXD, are candidate sites recognized by either a GDP/GTP release factor or a GTPase-affected protein.

Ras p21 participates as a molecular switch in the early steps of the signal transduction pathway that is associated with cell growth and differentiation (Bourne et al., 1990, 1991; Hall, 1990). When the protein is in its guanosine 5′-triphosphate (GTP)[1]-bound form, it is active in signal transduction, whereas in its GDP form it is inactive. The cycling between inactive and active conformations is mediated by exchange factors, or release factors, which increase the exchange rate of strongly-bound GDP with GTP (Downward, 1992; Lowy et al., 1991; Shou et al., 1992; Cen et al., 1992). The binding of GTP to ras p21 allows the molecule to present its effector domain in a conformation that can be recognized by both GTPase-activating proteins (GAP, NF1) and target effector molecule(s) (Martin et al., 1992; Lowy et al., 1991). The GTPase activity of ras p21 is considerably enhanced by binding of GAPs (Trahey & McCormick, 1987). The structure transition, called a "molecular switch", is vital to the proposed signal-transducing function of the protein.

X-ray crystallographic studies of GDP- and GTP-analogue-bound forms of H-ras p21 (Milburn et al., 1990; Schlichting et al., 1990) indicate that the conformational change is marked in residues 32–38 and 60–76. These two stretches of amino acids are on surface loops of the peptide, and are likely to have flexible and dynamic structures, subject to distortion in crystallization. At least two considerations raise the intriguing possibility that crystal structures reported for the GTP-bound form may not fully represent the conformation of the active form of this protein. The first is that the crystal structures show no GTP-induced change in conformation of the carboxy-terminal two-thirds of the polypeptide (i.e., residues distant from position 76), although there is biochemical evidence for the active and inactive state-dependent function of a distant portion of the molecule (Lowe et al., 1988; Willumsen et al., 1991). The second consideration arises from evidence that a portion of a different GTPase, cognate to the carboxy-terminal two-thirds of ras p21, mediates a critically important GTP-dependent effector function. This GTPase is the α chain of Gs; the GTP-dependent function is stimulation of adenylyl cyclase (Masters et al., 1988, 1990).

Changes in other regions of the protein may be too small to be detected by the methods used previously (Jurnak et al., 1990). Solution NMR spectroscopy provides structural information complementary to crystallography. Ligand-induced conformational change can be monitored by NMR spectroscopy as a function of ligand chemical structure and of residues comprising the binding site, and NMR chemical shifts are sensitive to the local environment.

In the present study, we have used heteronuclear-edited NMR methods to study the conformational change between GDP-bound and guanosine 5′-*O*-(3-thiotriphosphate) (GTPγS)-bound forms of human N-ras p21. GTPγS was chosen as a GTP analogue because of its high affinity for ras p21, approaching that of GTP, and because it is hydrolyzed by ras p21 at a reduced rate (Feuerstein et al., 1989), thereby functionally resembling GTP better than other GTP analogues. The crystal structure of ras p21 in this form has not yet been solved.

We have selectively labeled aspartic acid and asparagine (henceforth Asx) with ^{15}N in order to simplify the spectra. This approach was chosen because valuable information concerning the short-lived ras-GTPγS state (Feuerstein et al., 1989) could be obtained in a short time by taking advantage of the high sensitivity of ^{15}N-edited proton-detected methods (Griffey & Redfield, 1987). Asp residues are well dispersed

† This work was supported by USPHS Grant CA 51992. J.-S.H. was supported by a Samuel Goldwyn Fellowship and a Klein Fellowship from Brandeis University.

[1] Abbreviations: DTT, dithiothreitol; EDTA, ethylenediaminetetraacetic acid; EF-Tu, elongation factor Tu; GDP, guanosine 5′-diphosphate; GMPPNP, 5′-guanylyl imidodiphosphate; GNRF, guanine nucleotide release factor; GTP, guanosine 5′-triphosphate; GTPγS, guanosine 5′-*O*-(3-thiotriphosphate); HPLC, high-performance liquid chromatography; HMQC, heteronuclear multiple quantum coherence; HSMQC, heteronuclear single and multiple quantum coherence; IPTG, isopropyl β-D-thiogalactopyranoside; OD, optical density at 660 nm, A_{660}; NMR, nuclear magnetic resonance; NOE, nuclear Overhauser effect; PAGE, polyacrylamide gel electrophoresis; PMSF, phenylmethanesulfonyl fluoride; ppm, parts per million; SDS, sodium dodecyl sulfate; Tris, tris(hydroxymethyl)aminomethane; 1D, one dimensional; 3D, three dimensional.

0006-2960/93/0432-6763$04.00/0

in the sequence and located in almost all the important regions or motifs, and many are highly conserved in evolution (Valencia et al., 1991). In addition, the side chain carboxyl groups of Asp residues are involved in electrostatic interactions and hydrogen bonding networks, according to the crystal structure (Pai et al., 1990; Tong et al., 1991). Several of these side chains face toward, and are spatially very close to, the active site. We should expect that main chain NH, CO, and side chain COO(H) of Asp residues efficiently telegraph local enviromental changes. All these considerations should make amides of the Asp residues good reporters for studying the nucleotide-dependent conformational effects in ras p21.

Most of the data presented in this paper was taken on a variant of the native N-ras p21 that is truncated beyond residue 167. The truncated protein was chosen because the structure of similarly truncated H-ras p21 has been solved by X-ray crystallography and because the NMR spectrum of the truncated protein is slightly simpler than that of the full-length protein. Some data were also taken on the full-length protein, and those resonances which we observed that are common to both variants were unaffected, or only slightly shifted by the addition of the C-terminal chain (residues 168–189). Two further variants of the truncated protein, at residues 54 and 118, were also studied.

EXPERIMENTAL PROCEDURES

Materials. All ^{13}C- and ^{15}N-labeled amino acids were purchased from Cambridge Isotope Laboratories, except [1-^{13}C]glutamate, which was from Isotec. QA52 ion-exchange resin was from Whatman BioSystems Ltd., and Sephadex G-75 gel filtration resin was from Sigma Chemical Co. PD10 Sephadex G-25M columns were obtained from Pharmacia. Amicon membranes and Centricon microconcentrators were from Amicon. The colorimetric protein assay used was that of Bio-Rad.

Purification of GTPγS and HPLC Methods. GTPγS obtained from Boehringer Mannheim contains at least 5% GDP. We used QA52 ion-exchange chromatography to purify GTPγS to greater than 99% on the basis of HPLC chromatography before use for nucleotide exchange. HPLC was performed on an LC-18-DB column under ion-pairing conditions at a flow rate 1 mL/min. The elution buffer was 200 mM potassium phosphate, 4 mM tetrabutylammonium bromide, and 100 mM acetic acid (pH 6.7). This buffer gives elution times of 7.4 min for GDP and 11.2 min for GTPγS. HPLC was also used to monitor nucleotide substitution, binding, and NMR-based kinetics.

Bacterial Strains and Plasmids. DH5α was used as a host *Escherichia coli* strain (Hanahan, 1983) to fully label human N-ras p21 with $^{15}NH_4Cl$. When ras p21 was to be labeled with ^{15}N-labeled (and ^{13}C-labeled) amino acids, the polyauxotrophic strains of *E. coli* DL39 *avtA*::*Tn5* (*avtA*::*Tn5 aspC ilvE tyrB*; Muchmore et al., 1989; LeMaster & Richards, 1988) or another DL39 derivative, a mutant which has the conversion of Asp to Asn blocked (*asnA asnB*::*Tn5 aspC tyrB*; Muchmore et al., 1989), henceforth DL39 *asnA asnB*::*Tn5*, were used as previously described (Muchmore et al., 1989; Campbell-Burk et al., 1989). DL39 *avtA*::*Tn5* was used for labeling full-length ras p21 with [^{15}N]Asp, [^{15}N]Tyr, and [1-^{13}C]Val together, and [^{15}N]Asp and [1-^{13}C]Leu together, as well as for labeling a truncated variant C118S with [^{15}N]-Asp and [^{15}N]Gly. DL39 *asnA asnB*::*Tn5* was used for all other amino acid labeling of the truncated (1–167) cellular and the variant D54A N-ras p21.

The gene for full-length human N-ras p21 is carried on pTrc99C (Amann et al., 1988) and expressed under control of the trc promotor. The vector pTrc99C is a lac I^q and ampicillin resistance-bearing derivative of pKK233-2 (Amann & Brosius, 1985). The genes for truncated N-ras p21 and its variants, coding for residues 1–167, were similarly expressed from the trc promotor in pTrc99C. PCR techniques were used for site-directed mutagenesis. The mutagenic oligodeoxyribonucleotides for D54A and C118S are TGTTGG-TGTTGGCCATACTTGATACAG and AAACAAGA-GTAAACAAGAGTGATTTTCCAAC, respectively. These constructions were made by J. A. Noble, Onyx Pharmaceuticals.

Growth Conditions. M9 minimum medium (Muchmore et al., 1989) was used for the DH5α host strain. A highly supplemented medium was used for the polyauxotrophic strains of *E. coli* DL39 derivatives as previouisly described (Muchmore et al., 1989; Campbell-Burk et al., 1989); 50 mg/L Asn was used in the complementary media for the DL39 *asnA asnB*::*Tn5* cell line. The quantities of selectively labeled amino acids used in different preparations were 200 mg of Asp, 85 mg of Tyr, 115 mg of Val, 115 mg of Leu, 325 mg of Glu, 115 mg of Ile, 250 mg of Gly, 300 mg of Ala, and 210 mg of Lys per liter. Cells were grown and induced at 37 °C. Media containing labeled amino acids and 1 mM IPTG (final concentration) were inoculated to an optical density of approximately 0.8 with cells from similar cultures with unlabeled amino acids. The labeled cultures were harvested after overnight incubation for DH5α, 3–5 h for DL39 *avtA*::*Tn5*, and 6–10 h for DL39 *asnA asnB*::*Tn5*.

Purification of N-ras p21 Proteins. Harvested cells were disrupted by sonication in 50 mM Tris-HCl, pH 7.60, 10 mM $MgCl_2$, 50 mM NaCl, 5 mM DTT, and 1 mM PMSF. Generally, the majority of the full-length N-ras p21 was in the pellet, while in the case of truncated N-ras p21, 50% was in the sonication supernatant, and the rest was in the pellet. Both N-ras p21 in the supernatant and N-ras p21 in the pellet were purified separately, using methods similar to those described (Campbell-Burk et al., 1989; Redfield & Papastavros, 1990; Miller et al., 1992) with some modifications. The protein in the pellet was folded before purification. Both refolded ras p21 and supernatant ras p21 were purified by using two columns: ion-exchange chromatography on QA52 followed by gel filtration chromatography on Sephadex G-75. The final purity of the protein used for NMR experiments was greater than 98% as judged by gel scanning.

The sonication supernatant containing ras p21 was dialyzed against two changes of QA52 buffer (QA52 buffer: 50 mM Tris-HCl, pH 7.60, 20 mM NaCl, 5 mM $MgCl_2$, 1 μM GDP, 5 mM DTT, and 0.02% azide) for about 12-h intervals and was purified by QA52 ion-exchange chromatography with a total QA52 buffer volume of 900 mL of 20–300 mM NaCl gradient. Ras p21 was typically eluted in fractions with NaCl concentrations approximately from 190 to 220 mM for full-length ras p21 and from 210 to 240 mM for truncated ras p21. Fractions containing ras p21 were pooled and concentrated to approximately 5 mL, followed by gel filtration chromatography on Sephadex G-75. The protein purity after QA52 is about 60%.

The sonication pellet containing ras p21 was refolded before purification. The pellet was washed once in 30% sucrose and 5 mM EDTA (pH 7.60) and 3 times in 1% Triton X-100, 50 mM Tris-HCl (pH 7.60), 5 mM EDTA, and 4 mM DTT. The final pellet was resuspended in 30 mL of 7 M urea buffer (7 M urea, 50 mM Tris-HCl, pH 7.60, 5 mM EDTA, and 10 mM DTT), and protein was set at room temperature to be totally unfolded for 2–3 h.

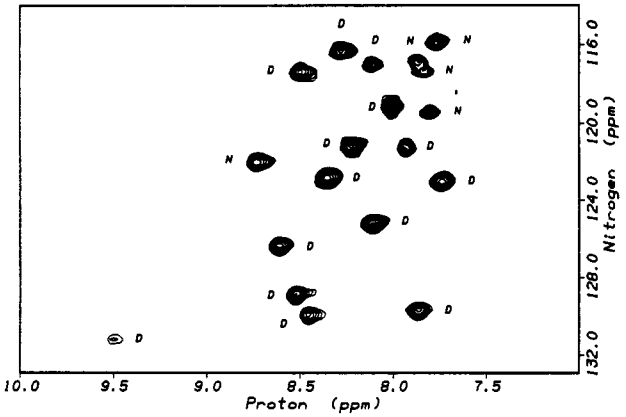

FIGURE 1: HSMQC spectrum of [^{15}N]aspartate-labeled truncated (1–167) N-ras p21, isolated from DL39 *AvtA*::*Tn5*, showing the resonances of the main chain backbone amides of both aspartates (14 residues, labeled with D) and asparagines (5 residues, labeled with N).

The supernatants containing ras p21 protein were diluted rapidly into a volume of 4 M urea buffer sufficient to produce a final concentration of 0.3 mg/mL (4 M urea buffer: 4 M urea, 50 mM Tris-HCl, pH 7.60, 5 mM $MgCl_2$, 50 μM GDP, and 2 mM DTT), to initiate folding of the protein with Mg^{2+} and GDP. The protein was refolded by dialyzing against gradually decreasing urea concentration in similar buffers, followed by QA52 buffer before QA52 ion-exchange chromatography. The purity of the protein was greater than 90%, as judged by gel scanning. Further purification was achieved by gel filtration chromatography on Sephadex G-75.

Ras p21 samples, folded by these methods, and also samples purfied directly from the soluble fractions bound approximately 1 stoichiometric equiv of GDP, GTPγS, or GMPPNP, and have intrinsic GTPase activity hydrolyzing GTPγS to GDP, based upon HPLC analysis. Both the soluble ras p21 and the refolded ras p21 give identical NMR spectra. Samples refolded in this way possess GAP-dependent GTPase activity similar to that of cytosolic ras p21 purified elsewhere.

Metal Substitution. Mg^{2+} bound to ras p21 was replaced with Mn^{2+} by chelation of Mg^{2+} bound to ras p21 and then addition of slightly substoichiometric amounts of Mn^{2+}; 0.5–1.0 μmol of ras p21 was dialyzed for 6 h at 4 °C against 400 volumes of 20 mM Tris-HCl, pH 7.6 at room temperature, 50 mM NaCl, 5 mM DTT, 10 μM GDP, 0.02% azide (Mg^{2+}-free NMR buffer), and 1 mM EDTA. Then the protein was dialyzed twice for 24 h against a similar buffer containing 100 μM $MnCl_2$ and twice against a Mg^{2+}-free NMR buffer containing 1 μM $MnCl_2$.

Exchange of Guanine Nucleotides. Replacement of bound GDP with GTPγS was achieved in Centricon tubes by using repeat dilution and concentration in the presence of both EDTA and high concentrations of GTPγS.

Approximately 1 μmol of GDP-bound ras p21 in 2 mL was incubated at room temperature with 4 μmol of EDTA and 4 μmol of GTPγS (purified before using, >99% as judged by HPLC) for 20 min and then concentrated to 0.5 mL. This procedure was repeated twice, with approximately 2 μmol of EDTA and 3 μmol of GTPγS for the second cycle and 0.5 μmol of EDTA and 2 μmol of GTPγS for the third cycle before reconcentration. After the last concentration, $MgCl_2$ and ^2H_2O were added to final concentrations of 5 mM Mg^{2+} and 10% ^2H_2O. The small amount of residual EDTA/Mg^{2+} did not affect NMR spectra or NMR-measured kinetics as shown by experiments where EDTA/Mg^{2+} was eliminated by passing through a PD10-G25 column. Nucleotide exchange was monitored by HPLC. Replacement of GDP by GTPγS was shown to be more than 92% complete by precipitation of ras p21 followed by HPLC, and the protein bound approximately 1 equiv of nucleotide(s). The immobilized alkaline phosphatase method (John et al., 1990) was also used to replace bound GDP with GTPγS. The two methods gave essentially the same result. Ras–GTPγS was shown to have the expected intrinsic GTPase activity by HPLC analysis and NMR (see results).

NMR Methods. NMR samples (10–20 mg) were prepared by dialysis against NMR buffer (NMR buffer: 20 mM Tris-HCl, pH 7.60, measured at room temperature, 50 mM NaCl, 10 mM DTT, 5 mM $MgCl_2$, 5 μM GDP, and 0.02% azide) and then concentrated in an Amicon concentrator using a YM10 membrane, followed by further concentration to about 0.36 mL in a Centricon tube. D_2O was added to 10% for NMR lock.

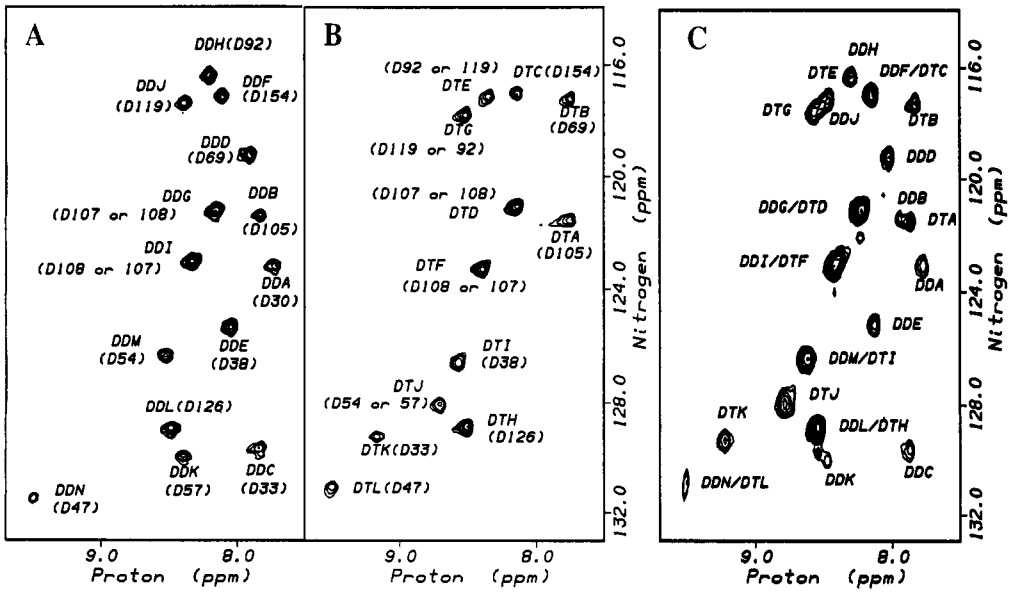

FIGURE 2: Comparison of [^{15}N]aspartate-labeled truncated human N-ras p21 in the GDP- and GTPγS-bound forms. HSMQC spectra of the amides are shown. (A) GDP-bound form at 5 °C; (B) GTPγS-bound form at 5 °C; (C) when ras-GTPγS is partially hydrolyzed, the resonances from both GDP- and GTPγS-bound forms are simultaneously dectected; the spectrum was acquired at 15 °C.

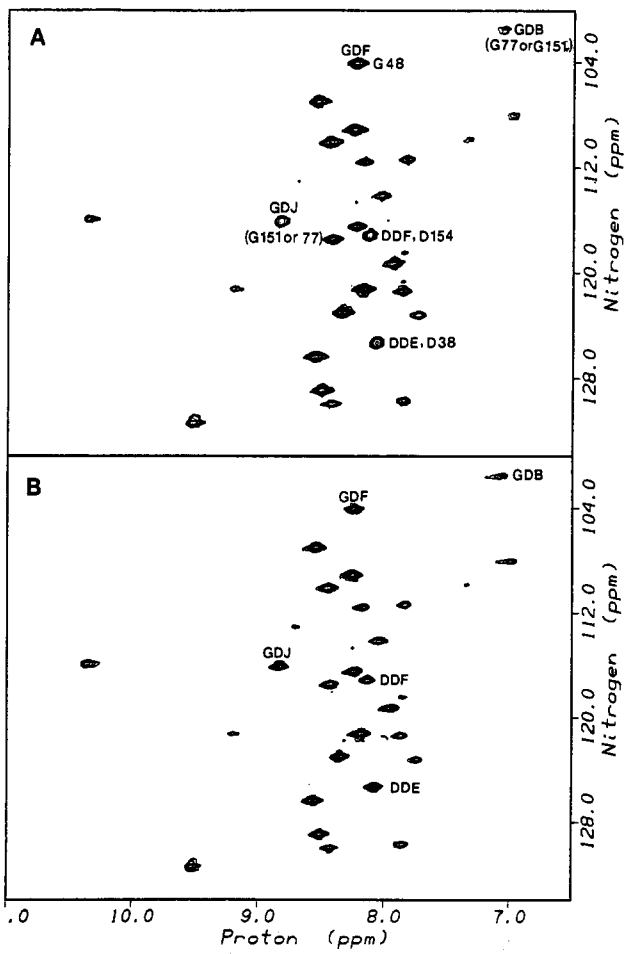

FIGURE 3: Comparison of [^{15}N]aspartate-, [^{15}N]glycine-, and [1-^{13}C (carbonyl)]glutamate-labeled truncated N-ras p21 in the GDP state, with and without decoupling ^{13}C. HSMQC spectra of selected amides in the GDP-bound state at 5 °C are shown. (A) The spectrum was taken without decoupling the carbonyl ^{13}C; (B) the spectrum was taken with decoupling. Couplings between amide nitrogens and ^{13}C-enriched carbonyl carbons are seen as 15-Hz splittings or broadenings in the ^{15}N dimension that are abolished by decoupling ^{13}C.

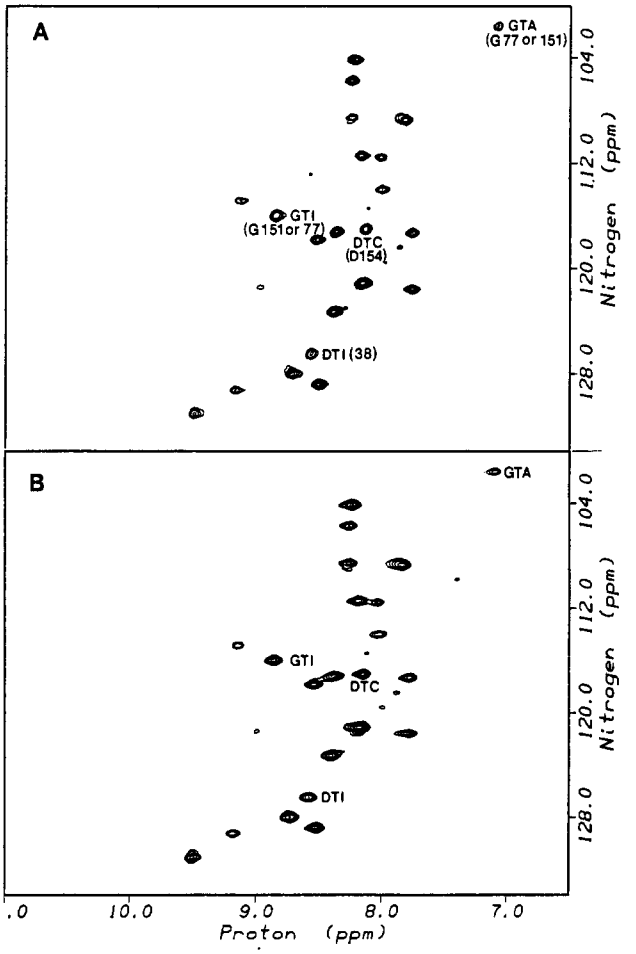

FIGURE 4: Comparison of HSMQC spectra of [^{15}N]aspartate-, [^{15}N]-glycine-, and [1-^{13}C (carbonyl)]glutamate-labeled truncated N-ras p21 in the GTPγS state at 5 °C, with and without decoupling the carbonyl ^{13}CO. (A) Spectrum was taken with no carbonyl decoupling; (B) spectrum was taken with carbonyl decoupling.

Two-dimensional ^{1}H, ^{15}N correlation spectra were obtained as described previously with JR water suppression (Campbell-Burk et al., 1989) on a custom-built 500-MHz spectrometer and on a Bruker AMX 500 instrument.

Spectra were collected at 5, 15, 25, and 37 °C to establish small corrections to chemical shifts. Data were analyzed with minor preweighting to reduce noise from H_2O, and spectra were plotted using software kindly supplied by Hare Software (Woodinville, WA). ^{1}H chemical shifts are relative to that of H_2O at 4.80 ppm, and ^{15}N chemical shifts are relative to neat $^{15}NH_3$. Differences in chemical shifts between spectra of samples prepared from different cultures and collected on different days are approximately 0.01 ppm ^{1}H and 0.1 ppm ^{15}N.

RESULTS

Asp Resonances in GDP- and GTPγS-Bound Forms and Nucleotide-Dependent Conformational Change of Human N-ras p21. Heteronuclear-edited proton-observed two-dimensional ^{1}H, ^{15}N correlation, either HMQC (heteronuclear multiple quantum coherence) or HSMQC (heteronuclear single and multiple quantum coherence), methods were used to generate two-dimensional spectra of [^{15}N]Asx-enriched protein (Figure 1). By observing changes in the chemical shifts, or in the intensities of the resonance peaks, we expect to obtain a qualitative picture of structural and dynamic changes.

The auxotrophic strain DL39 *avtA*::*Tn5* was used to label Asp and Asn simultaneously (Figure 1) and resolve nearly every Asx amide resonance in the GDP-bound form of truncated human N-ras (1–167), and most Asx resonances in the GTPγS-bound form (data not shown). To further simplify the spectra, the auxotrophic strain DL39 *asnA asnB*::*Tn5* was used to selectively label Asp without Asn (Figure 2A). One of the resonances, DTB, in the GTPγS form (Figure 2B), which has identical chemical shifts to one of the Asn residues in the GDP-bound form (Figures 1 and 2B), is thereby clearly resolved. Of the 14 Asp resonances in the GTPγS form, 12 are well resolved (Figure 2B).

To assign these peaks to specific amino acid residues, several further methods were used: Several protein samples were labeled with both [^{15}N]Asp and one other amino acid labeled with ^{13}C at its carbonyl (CO) position. The latter was chosen to be one of the amino acids which precedes an Asp residue. The directly-bonded ^{13}C nucleus, which has a nuclear spin of $^{1}/_{2}$, splits the resonances of the following Asp residue(s) in the ^{15}N dimension (Figures 3 and 4). This splitting (of about 15 Hz) is generally confirmed by observing its removal when the carbonyl (^{13}CO) resonance is decoupled [see, for example, Campbell-Burk et al. (1989)]. When this method was ambigous, we used a variety of strains, mutations, and ligands to perturb or eliminate specific classes of Asp resonances, or perturb the protein locally as judged by the NMR spectrum.

Table I: ^{1}H and ^{15}N Chemical Shifts (ppm) Observed in the Truncated (1–167) Human N-ras p21 in the GDP-Bound Form at 5 °C

resonance	assignment	chemical shifts (ppm) ^{1}H	^{15}N
DDA	Asp-30	7.75	123.2
DDB	Asp-105	7.86	121.4
DDC	Asp-33	7.87	129.8
DDD	Asp-69	7.94	119.3
DDE	Asp-38	8.09	125.4
DDF	Asp-154	8.15	117.2
DDG	Asp-107, -108[a]	8.20	121.2
DDH	Asp-92	8.24	116.4
DDI	Asp-108, -107[a]	8.37	123.1
DDJ	Asp-119	8.45	117.5
DDK	Asp-57	8.44	130.1
DDL	Asp-126	8.52	129.0
DDM	Asp-54	8.57	126.4
DDN	Asp-47	9.56	131.4
NDA	Asn-172[b]	8.05	118.7
GDB	Gly-77, -151	7.07	101.6
GDJ	Gly-151, -77	8.84	116.2
GDF	Gly-48	8.25	104.3

[a] These assignments are based upon elimination and collectively assigned. [b] The chemical shifts are from wild-type full-length N-ras p21.

Table II: ^{1}H and ^{15}N Chemical Shifts (ppm) for Aspartate and Glycine Resonances of the Truncated Human N-ras p21 in the GTPγS-Bound Form at 5 °C

resonance	assignment	chemical shifts (ppm) ^{1}H	^{15}N
DTA	Asp-105	7.76	121.6
DTB	Asp-69	7.76	117.3
DTC	Asp-154	8.16	117.1
DTD	Asp-107, -108[a]	8.16	121.1
DTE	Asp-92, -119[a]	8.36	117.2
DTF	Asp-108, -107[a]	8.40	123.3
DTG	Asp-119, -92[a]	8.54	117.9
DTH	Asp-126	8.52	129.0
DTI	Asp-38	8.58	126.6
DTJ	Asp-57, -54[b]	8.72	128.1
DTK	Asp-33	9.19	129.3
DTL	Asp-47	9.53	131.1
NTA	Asn-172[c]	8.04	118.8
GTA	Gly-77, -151	7.08	101.7
GTI	Gly-151, -77	8.84	116.1

[a] These assignments are not rigorous, but are tentatively paired with the GDP-form resonances closest to them in chemical shifts. [b] This resonance is rigorously assigned to either Asp-54 or Asp-57, but we do not know which one. We have not found the other resonance corresponding to these two residues in the GTPγS form. [c] The chemical shifts are from wild-type full-length N-ras p21.

Crystallographic data indicate that when GTPγS is substituted for GDP in truncated cellular H-ras p21, about 28 residues out of 166 (17%) appear to change their local conformation. In contrast, the NMR spectra indicate that a larger portion of Asp residues (over 60% as judged by their changes in NMR shifts) experience a different environment at approximately physiological conditions. Resonance shifts greater than the line width of the amide H or N (40 Hz in ^{1}H and 25 Hz in ^{15}N dimensions) are interpreted to indicate a local change. Figure 2 compares spectra of GDP- and GTPγS-bound truncated N-ras p21 selectively labeled with [^{15}N]aspartate. Tables I and II list assignments achieved in this work.

We were concerned that excess Mg^{2+} ions in solution might form coordination complexes with carboxylates of Asp side chains, in addition to the tight Mg^{2+}-binding site, which could influence the chemical shifts of some Asp amide groups. A titration experiment, varying the Mg^{2+} concentration from 1 to 10 mM, was performed on both GDP- and GTPγS-bound ras p21 (1.5 mM) complexes (data not shown). None of the Asx chemical shifts change over this range of Mg^{2+} concentration. A kinetic experiment showed that when the nucleotide GTPγS, bound to ras p21, is completely hydrolyzed over many days, the HSMQC spectrum of the resulting GDP-ras p21 + P_i is exactly the same as the original spectrum of GDP–ras p21 (data not shown) and that when GTPγS is partially hydrolyzed resonances from both GTPγS- and GDP-bound forms are simultaneously visible (Figure 2C).

Resonance Assignments in both the GDP- and GTPγS-Bound Forms. Since ^{32}Tyr-^{33}Asp, ^{46}Ile-^{47}Asp, and ^{68}Arg-^{69}Asp are unique sequential pairs in N-ras p21, these Asp assignments were relatively easy by means of double ^{13}C–^{15}N labeling as mentioned above. Three samples were produced, all labeled with ^{15}N-enriched Asp, and each labeled with a single [^{13}C]carbonyl-enriched amino acid. The three ^{13}C-enriched amino acids were Tyr, Ile, and Arg, and the HSMQC spectra of each doubly labeled protein showed a single Asp resonance which was slightly split by the neighboring ^{13}C label, thereby uniquely identifing the resonances Asp-33, -47, and -69. These samples were then converted to the GTPγS-ligated form, and the splittings were again observed, in order to achieve assignments in that form as well. Both Asp-33 and Asp-69 were responsive to the change in ligand, while Asp-47 was not. Asp-69 moves to a position occupied by one of the Asn resonances in the GDP-bound form (Figures 2B and 1).

When two or more aspartate residues are preceded by the same amino acid, aspartate assignments were achieved using the same double-label methods in conjunction with further experiments. For example, Asp-38, the only conserved residue in β2, is essential for GAP binding to ras p21 (Calés et al., 1988). To identify and study it, we labeled ras p21 with [1-^{13}C]-Glu and [^{15}N]Asp (Figures 3 and 4). For this sample, as for some others in this research, [^{15}N]Gly was also incorporated because its resonances are well characterized (Redfield & Papastavros, 1990; Campbell-Burk, 1989; Miller et al., 1992) and do not overlap with those of [^{15}N]Asp. Glu precedes both Asp-38 and Asp-154. It was easy to pick out Asp-38 and Asp-154 in a high-resolution HSMQC spectrum from splittings in their ^{15}N dimension, by [1-^{13}C]Glu, which disappeared upon ^{13}CO decoupling in both the GDP and GTPγS forms (Figures 3 and 4). This experiment rigorously identifies the resonances of Asp-38 and Asp-154 with peaks DDE and DDF for the GDP form, and with peaks DTC and DTI for the GTPγS form, but does not indicate which peak belongs to which residue. However, two resonances (DDF and DTC) are in exactly the same position in the spectra of the GDP and GTPγS forms, while the other two (DDE and DTI) are separated by about 0.5 ppm in the ^{1}H dimension, and are far from DDF/DTC. It is expected that the largest spectral perturbations produced by GTPγS substitution come from residues closest to the nucleotide, so we assign the apparently unshifted resonances DDF and DTC to Asp-154, which is remote from the nucleotide site, and the other pair of resonances to Asp-38 (Figures 3 and 4).

These assignments were further confirmed by a Mn^{2+} substitution experiment by taking advantage of the fact that the amide (NH) of Asp-38 is much closer to the metal than is that of Asp-154 [7.7 and 19.5 Å, respectively, from nitrogen, based upon Schlichting et al. (1990)]. A [^{15}N]Asp-labeled sample was prepared for which the tightly bound Mg^{2+} was replaced by the paramagnetic ion Mn^{2+} (Figure 5). As discussed in detail elsewhere (Miller et al., 1992), the paramagnetic Mn^{2+} ion is expected to wipe out resonances of

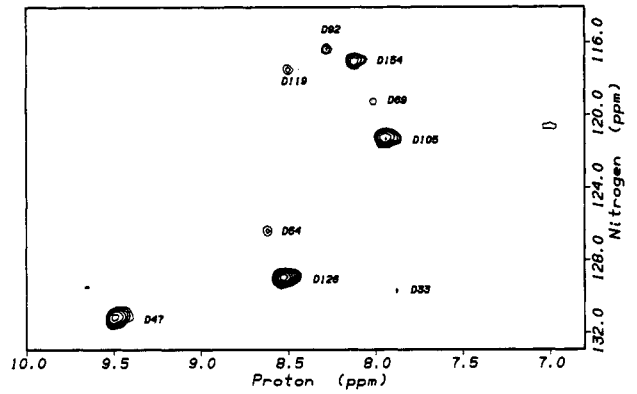

FIGURE 5: HMQC spectrum of [^{15}N]aspartate-labeled truncated N-ras p21 in the GDP-bound form containing Mn^{2+} taken at 15 °C. A number of strong peaks due to residues more than 23 Å from the metal are labeled as well as a less intense group of resonances from residues that are between 15 and 17 Å from the metal.

amides within a distance of the order of 15 Å. In Figure 5, only one of two resonances, assigned to residues Asp-154 and Asp-38, remains intense, and this resonance must be that of the more distant Asp-154; a number of other residues that are distant from the metal are also seen.

It was especially important to identify resonance DTI with Asp-38, because this GTPγS-bound form resonance is in the same position as resonance DDM in the GDP-bound form. These two resonances do not come from the same residue, as might have been assumed; DDM is assigned to Asp-54 (see below).

In the spectrum of Figure 3, two glycine peaks are broadened by the ^{13}CO label. Of these, one must come from Gly-77, while the other comes from Gly-151 that is preceded by Gln, which co-labels with Glu (Muchmore et al., 1989). Both are rigorously shown to be unresponsive to GTPγS substitution (Figures 3 and 4). We have also identified resonance GDF with Gly-48 by means of 1D and 3D isotope-aided NOE (Campbell-Burk et al., 1989; Clore & Gronenborn, 1992) to Asp-47 (data not shown).

Similar methods that were used to identify Asp-38 and Asp-154 were used for Asp-30 and Asp-126. A [1-^{13}C]Val, [^{15}N]Asp, and [^{15}N]Tyr triply labeled wild-type full-length sample was prepared for this purpose.

The invariant Asp-57 is in the nucleotide-binding ^{57}DXXG motif, and its side chain is in the metal-binding site. Asp-54 is in the antiparallel β3-sheet, near a region previously reported to be sensitive to substitution of GTPγS for GDP (Yamasaki et al., 1989). A full-length protein labeled with [1-^{13}C]Leu and [^{15}N]Asp was produced. Three peaks were found to have ^{13}C splittings in GDP-ligated protein, and one of these was unresponsive to nucleotide. This resonance was unambiguously identified with Asn-172 because it was lacking in spectra of the truncated protein. The other two resonances, DDK and DDM, are thus rigorously assigned to residues Asp-57 and Asp-54. Finally, we assign residue Asp-54, which is 16.5 Å from the metal, to DDM and Asp-57 to DDK because a peak at this position is still clearly observable, although weakly, in a Mn^{2+}-substituted sample (Figure 5). Asp-57 is only 7.7 Å from the metal and is expected to be wiped out by the Mn^{2+} electronic spin.

In the GTPγS-bound form of this sample, we have found only one Asp resonance that is definitely split by the ^{13}CO label, namely, resonance DTJ. We do not have any criterion for assigning it to either possible residue Asp-54 or Asp-57, at this time. Nevertheless, both Asp-54 and Asp-57 clearly have a nucleotide-dependent shift of at least 0.28 ppm in ^{1}H and 2.0 ppm in ^{15}N dimensions. It is also possible that one could be shifted and the other broadened beyond detection.

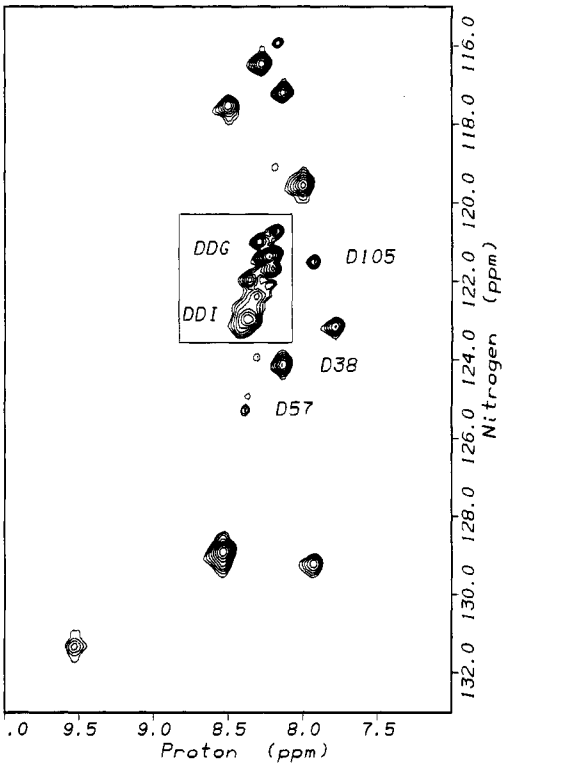

FIGURE 6: HSMQC spectrum of truncated D54A mutant labeled by [1-^{13}C]Leu and [^{15}N]Asp in the GDP-bound form at 15 °C. The box contains a cluster of resonances including Asp-107 and -108 from correctly folded protein, and other residues which probably arise from incorrectly folded protein.

Table III: Comparison of ^{1}H and ^{15}N Chemical Shifts (ppm) for Resonances of Truncated Human Cellular N-ras p21 and Mutants in the GDP-Bound Form at 5 or 15 °C[a]

	chemical shifts (ppm)					
	wild type		D54A		C118S	
residue	^{1}H	^{15}N	^{1}H	^{15}N	^{1}H	^{15}N
Asp-119	8.43	117.5[b]			8.33	116.9[b]
Asp-38	8.09	125.4	8.16	124.1		
Asp-57	8.44	130.1	8.38	125.3		

[a] Only residues which appear sensitive to the mutation are included. [b] These data were obtained at 5 °C.

In an attempt to further confirm the identifications of Asp-57 and Asp-54, we labeled a truncated D54A mutant N-ras p21 with [1-^{13}C]Leu and [^{15}N]Asp (Figure 6). Surprisingly, the resonance assigned to Asp-57 is shifted in the GDP form, as is the resonance assigned to Asp-38 in the effector region (Table III). The spectrum shows a cluster of extra peaks which could be due to a denatured fraction of protein, at around resonances Asp-107 and Asp-108, 8.18–8.37/120.7–123.0 (^{1}H/^{15}N dimensions) ppm. However, resonances beyond Asp-38 and Asp-57 are found in their normal positions (Figure 6). Although the experiment has not led to confirmation of the Asp-57 identification, it demonstrates the importance of this fragment of antiparallel β-sheet.

GTPγS-Induced Conformational Effects in the Second Domain of ras p21. Comparing the HSMQC spectrum of the GTPγS state with that of the GDP form of ras p21 (Figure 2), we have discovered that there are more resonances which are responsive to changing bound nucleotide. Thus, we have extended our assignments to further residues, the second

domain of the protein (residues distant from Glu-76), in addition to those already discussed.

To identify the resonance of Asp-119, a C118S mutant of truncated N-ras was labeled with [^{15}N]Asp and [^{15}N]Gly. All of the resonances in the GDP form appeared to be in the same place as in the cellular protein, except for resonance DDJ, which was slightly shifted (Table III), and we have therefore assigned it to Asp-119 because it is next to the mutation point in the primary amino acid sequence. Upon replacement of GDP by GTPγS, this resonance, Asp-119, is clearly shifted (Tables I and II).

Asp-92 links two short α helices, α3 and α3′, in the GMPPNP form (Pai et al., 1990) but is a member of the continuous α-helix α3 in the GDP form (Tong et al., 1991). We have identified Asp-92 by labeling ras p21 with [1-^{13}C]-Ala and [^{15}N]Asp. Asp-92 is clearly responsive to nucleotide substitution although we have not yet unambiguously assigned its resonance in the GTPγS-bound form (Tables I and II).

Asp-105, a residue in loop 7 (L-7), is also in the second domain of the protein. We have only assigned Asp-105 in an Asp-12 oncogenic mutant both in the GDP and in the GTPγS forms by incorporating [1-^{13}C]Lys and [^{15}N]Asp into the G12D mutant N-ras p21. Since the chemical shifts of this peak, like those of most of the other Asp resonances in the G12D mutant, are identical to the wild-type shifts (data not shown), we assume its identification is valid for wild-type ras p21. Asp-105 is also sensitive to nucleotide exchange.

Finally, the collective identification of Asp-107 and Asp-108 is by elimination, since all other Asp residues are assigned. Their resonances appear to be unresponsive to nucleotide substitution.

Note: After the present work was completed, assignments of the backbone resonances of the GDP-bound form of truncated H-ras p21 became available (Campbell-Burk et al., 1992; Muto et al., 1993). Our assignments of the GDP-bound form in truncated N-ras p21 seem to be consistent with these assignments in H-ras p21.

DISCUSSION

By comparison of Asp ^{15}NH shifts in GDP- versus GTPγS-ligated truncated N-ras p21, we can infer the relative size of conformational changes in the protein due to nucleotide substitution (Tables I and II). We find large differences in chemical shifts at residues Asp-30, Asp-33, Asp-38, Asp-54, Asp-57, and Asp-69, and virtually no differences at residues Asp-47, Gly-48, Gly-77, Asp-107, Asp-108, Asp-126, Gly-151, Asp-154, and Asn-172. Most interestingly, there are relatively smaller but distinct differences at three residues, Asp-92, Asp-105, and Asp-119, in the second domain of ras p21. The positions of these NMR markers in the X-ray structure are shown in Figure 7.

These observations demonstrate the high sensitivity of the Asp probe, presumably resulting in part from hydrogen bonding and electrostatic interaction networks of its side chain. A comparison of the GDP- and GTP-bound states of X-ray models (Schlichting et al., 1990; Milburn et al., 1990) indicates that differences between the two states are confined to the areas of residues 32–38 and 60–76, which have been called the switch I and switch II regions. It seems unlikely that the large and complex α/β structure beyond residue 76 is entirely insensitive to the species of nucleotide bound, as the current X-ray results seem to imply. The second domain could

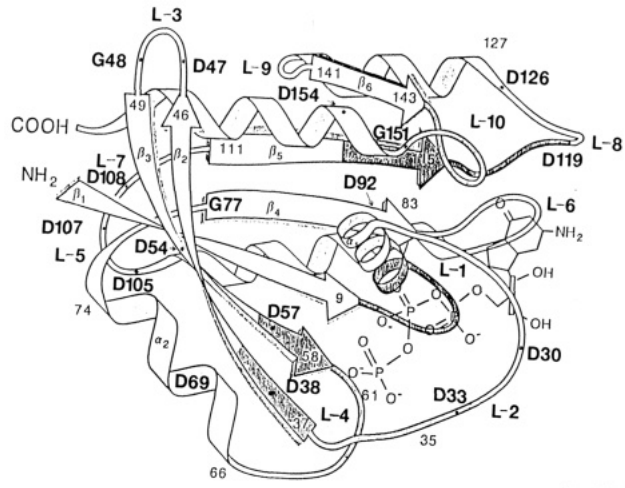

FIGURE 7: Ribbon diagram of truncated human Ha-ras p21 (1–166), showing the positions of several of the markers discussed in the text [adapted from Bourne et al. (1991)].

participate in regulating the exchange of guanine nucleotides and effector function.

In the present studies, we have used isotope-editing NMR methods in conjunction with selective [^{15}N]aspartate labeling to obtain greatly simplified spectra. Individual assignments were made of most of the Asp ^{15}NH peaks, as well as one Asn residue and three Gly resonances, using ^{13}C double labeling and other methods, in both the GDP- and GTPγS-bound forms under approximately physiological conditions (Tables I and II). In several cases, it was important to perform rigorous assignments using double labeling of neighboring amino acids in both ligand states, because of resonance interchanges that would otherwise have been confusing.

Titration of the Mg^{2+} concentration for both N-ras p21–nucleotide complexes tends to rule out the possibility of weak Mg^{2+}-binding sites which could lead to misleading results. The chemical shift differences produced by GTPγS are reversible in the sense that, as GTPγS is hydrolyzed over several days, the GDP-bound form resonances reappear (Figure 2C).

We now discuss the significance of these observations for each region of the molecule.

Effector-Binding Region. Amino acids 32–40 have been shown to be involved in the binding of GAP (Adari et al., 1988; Calés et al., 1988). Distinct chemical shift changes of Asp-33 (660 Hz in the ^{1}H dimension) and Asp-38 (245 Hz in the ^{1}H dimension and 60 Hz in the ^{15}N dimension) indicate that substantial structural changes may occur in this region upon replacement of GDP by GTPγS. These are two of the biggest chemical shift changes which have be identified by NMR in this protein. The large magnitudes of these chemical shift changes could be interpreted to show that conformational changes in this region are significant (Schlichting et al., 1990).

As a reporter in the switch II region, Asp-69 clearly demonstrates that there is also a comformational switch in this region. The switch II and switch I regions both contact the nucleotide and are located close to each other where they can easily interact with GAP (Pai et al., 1990).

Metal-Binding Site. There is some contradiction in the reports of the precise nature of the Mg^{2+}-binding site. The major difference between two X-ray models near the metal lies in Asp-57 in the GDP-bound form. Schlichting et al. (1990) find that, when the GDP state is created after hydrolysis of a caged form of GTP, the Mg^{2+} appears to lose an intervening water ligand and acquire the carboxylate of Asp-

57 as a ligand. Another crystallography study (Tong et al., 1991) shows that, in GDP–ras p21, the Mg^{2+} ion is coordinated by O atoms from the β-phosphate of GDP, Ser-17, and four water molecules. Two of these water molecules appear to interact with the side chain of Asp-57 and the main chain of Asp-33, respectively. Electron paramagnetic resonance studies of a ras $p21_{EJ}$–Mn^{2+}–GDP complex show that four water molecules coordinate to the metal ion together with an O from the β-phosphate group and one O from the protein (Latwesen et al., 1992), apparently in agreement with Tong et al (1991). However, studies of crystals of Mn^{2+}–H-ras p21 indicate that the protein conformation is different from that of Mg^{2+}–H-ras p21 (Wittinghofer & Pai, 1991).

Mg^{2+} could mediate the conformational change considering the fact that Mg^{2+} moves slightly in different states (Schlichting at al., 1990). When GTPγS is substituted for GDP, we found that the amide proton of Asp-33 shifts down field 1.32 ppm, which is one of the most dramatic shifts detected in ras p21. Asp-57 is also shifted significantly both in ^1H and in ^{15}N frequencies. Although our data on Asp-57 and Asp-33 favor the model of Schlichting et al. (1990) regarding the change of Asp-57, they could not be fully explained by it. In the crystal structure of H-ras p21–GMPPNP, Asp-57 is completely rigid (Pai et al., 1990). It is unlikely that the nucleotide-dependent amide perturbation of Asp-57 is solely the result of movement of Mg^{2+}, which might influence its side chain's coordination distance to Mg^{2+}. Thus, the distinct chemical shift changes in Asp-57 (minima of 140 and 100 Hz in the ^1H and ^{15}N dimensions, respectively) must be due to, and an indication of, some other change(s) at this position. This part of the β-sheet (around Ser-39 and Leu-56) has been reported to be changed upon replacement of GDP by GTPγS (Yamasaki et al., 1989), which appears to contradict the crystal data. It is of interest that we find that the chemical shift of Asp-54 is nucleotide-dependent (Tables I and II). A change in the β-sheet extending as far as Asp-54 has not been indicated previously and is not entirely expected.

If the main chain carbonyl of Asp-33 is indirectly coordinated to the Mg^{2+} ion in both the GDP and GTPγS forms, then we propose that the dramatic changes noted above in the chemical shifts (1.32 ppm in the ^1H dimension) of Asp-33 should be the result of several changes in the effector-binding region and the metal-binding site. The major contributions to these changes of Asp-33 could come from nucleotide-dependent reorientation of its side chain, metal perturbation, and change of the interactions in this part of the effector region, especially the "flip peptide YDP" region (Schlichting et al., 1990).

Guanine Nucleotide-Binding Pockets. According to the crystal structures, Asp-30 appears to be involved in weak hydrogen bonds to the ribose 2,3-hydroxyls through its side chain carboxyl group in the GMPPNP form. Crystallographic studies do not predict nucleotide-linked effects within this fragment of polypeptide. Changes in this region are nevertheless expected considering that determinants within residues 17–32 may be important for ras binding to GAP (Schaber et al., 1989). We find that the Asp-30 resonance is nucleotide-sensitive. Its resonance in the GTPγS state has not been located, and it is either broadened beyond detectability or else shifted at least 1.6 ppm in the ^{15}N dimension. From this observation, we infer that the ribose conformation or orientation is disturbed somehow. As a consequence, the guanine ring has to be reorientated to accommodate this change.

If this proposal is correct, we would expect that Asp-119 is responsive to the reorientation of the guanine base ring, because the carboxylate group of Asp-119 makes two hydrogen bonds to the guanine base (Pai et al., 1990). Upon replacement of GDP by GTPγS, the Asp-119 ^{15}NH is clearly shifted, but not dramatically, as is expected.

The ^{116}NKXD guanine base-binding motif connects the phosphate-binding loop through strong hydrogen bonds to Gly-13 and Val-14 (Pai et al., 1990). Changes which we observed in the phosphate-binding loop further support the proposal. In a spectrum of uniformly ^{15}N-labeled protein, the two peaks previously identified with Gly-13 and Lys-16 at around 10.5 ppm in the GDP form (Redfield & Papastavros, 1990) are no longer visible, and are shifted upfield in the GTPγS form at least 1 ppm (protons; data not shown).

Potential Binding Sites for Guanine Nucleotide Release Factor (GNRF). A critical step in signal transduction (Szeberenyi et al., 1990) is to accumulate the active, GTP-bound form of ras proteins in cells. To reach the active GTP-bound state, ras proteins must first release bound GDP. This rate-determining step in GTP binding is thought to be catalyzed by a GNRF (Wolfman & Macara, 1990; Downward, 1992; Shou et al., 1992; Cen et al., 1992; Martegani et al., 1992). Understanding the ras–GNRF interaction will enhance our knowledge of many signal transduction pathways mediated by ras proteins.

It has been suggested that the binding site of GNRF is not located in either switch region, or in the phosphate-binding loop, but that regulatory elements such as these regions can influence the ras p21 response to GNRF (Mistou et al., 1992; Bourne et al., 1991). The purified carboxy-terminal domains of SCD25 and GST–$p55^{ras}$–GNRF (Créchet et al., 1990; Shou et al., 1992) promote the release of both GDP and GTP from ras p21. However, the ras–GDP complex is the preferred target; the dissociation of GDP by GNRF is more strongly accelerated than that of GTP. We would therefore expect that there are some nucleotide-dependent structural differences in ras p21 that could be recognized by GNRF. It does not seem possible to predict a GNRF-binding site based upon the crystal structure differences between the GTP and GDP states. It is likely that some exposed structural elements, besides the switch regions and the phosphate-binding loop, of the molecule may be involved in GNRF recognition.

Our results on the GTPγS-induced conformational change might define a number of possible regions as potential targets of GNRF action. The first is the region approximately from Asp-92 to Asp-105. Both Asp-92 and Asp-105 amide chemical shifts are affected upon replacement of GDP by GTPγS. This region is spatially close to the end of the switch II region (Verrotti et al., 1992) and the L-8 region in the crystal structure, but is not present in EF-Tu (Valencia et al., 1991); thus, this cluster could interact with GNRF. Residues 103–108 may take part in the activation by GNRF, as suggested by Willumsen et al. (1991). They showed that mutations of residues 102 and 103 abolish the biological functions of ras p21, an effect possibly associated with an altered GNRF interaction.

The second region is around Asp-119, in the L-8 region. The GTPγS-induced differences in the structure of this region are candidates for structural determinants required for molecular recognition. It is also proposed, by comparison of the structural and functional properties of p21 and EF-Tu or G protein α subunits, that L-8 could be involved in the binding of GNRFs (Bourne et al., 1991; Valencia et al., 1991). One could speculate that dissociation of bound nucleotide requires loosening of protein–base contacts in L-8 and other regions, brought about by the interaction of these loops with GNRF.

Carboxyl Terminus. We have shown that the amides of Gly-151, Asp-154, and Asn-172 in the carboxyl region are insensitive to nucleotide exchange (Tables I and II); thus, it is unlikely that the GTPγS-induced conformational changes extend beyond Gly-151. It is interesting that the carboxy-terminal region of ras p21 does not interact with the nucleotide exchange factor SDC25 C-domain (Mistou et al., 1992). However, it is possible that different ras proteins may be controlled in different ways (Mizuno et al., 1991; Hata et al., 1991), because both posttranslational modifications and phosphorylation by protein kinases take place in the C-terminus. The proton chemical shift of Asn-172 is not in the expected random-coil range for this amino acid (Wüthrich, 1986). This, and the normal appearance of this resonance, suggests that the C-terminus (at least up to Asn-172) has a folded structure, though not necessarily one that contains α-helixes or β-sheets.

CONCLUSIONS

We have added NMR-based indications of conformational changes to information from X-ray crystallographic studies, and have observed effects on residues distant from the active site. This information leads us to propose a working model for the conformational change.

Asp-47 and Gly-48 are conserved interface residues; they are not present in EF-Tu (Valencia et al., 1991). These residues and Gly-77 are not far from the sequence-variable C-terminal specificity region involved in membrane attachment. The resonances of Asp-47, Gly-48, and Gly-77 are not sensitive to nucleotide exchange, and that of Asp-47 is also insensitive to metal substitution (we see its resonance unshifted in Mn^{2+}-substituted N-ras p21). Residues Asp-47 and Gly-48 comprise loop 3, which links the sole antiparallel β-sheet in ras p21. The insensitivity of this loop to ligand replacement suggests that the part of the antiparallel β-sheet nearest to it is especially rigid. The entire β-sheet could be a hinge, the part nearest to loop 3 being a rigid pivot, and distal parts being a movable part of the hinge during the process of conformational change as also suggested by NOESY studies of Yamasaki et al. (1989). The fact that the D54A point mutation perturbs the conformation of ras p21 in limited regions, especially at Asp-57 in this β-sheet, as well as at Asp-38 in the effector region, demonstrates the importance of this fragment of β-sheet.

We have demonstrated that the second domain conformation is sensitive to the nucleotide species. Thus, we propose that motion of the ribose and the guanine base may mediate the conformational effects of ras p21, and bridge the ^{116}NKXD L-8-binding motif with the effector-binding region (through Asp-30) as well as the phosphate-binding loop (through both Val-14 and Gly-13). Gly-77 may also play a role as a second hinge which links the first and the second domain and mediates the conformational changes in both domains. Our results also imply a role for Asp-92 in the conformational switch of the region from Asp-92 to Asp-105.

On the basis of this working model, we predict conformational changes in several regions. These include, for example, the antiparallel β-sheet regions beyond Arg-41 and Asp-54, which link to switch regions, and the L-10 ^{143}ETSAK motif which weakly binds to the guanine base, as well as other residues in the guanine nucleotide-binding pockets.

ACKNOWLEDGMENT

We thank F. McCormick and J. A. Noble for providing ras plasmids, M. Papastavros for advice and assistance, F. W. Dahlquist and E. Anderson for the gift of *E. coli* strains, C. J. Halkides for help with HPLC and with the alkaline phosphatase methods for nucleotide exchange, and T. Yang for preparing the labeled mutant variant C118S N-ras p21 sample.

REFERENCES

Adari, H., Lowy, D. R., Willumsen, B. M., Der, C. J., & McCormick, F. (1988) *Science 240*, 518–521.
Amann, E., & Brosius, J. (1985) *Gene 40*, 183–190.
Amann, E., Ochs, B., & Abel, K.-J. (1988) *Gene 69*, 301–315.
Bourne, H. R., Sanders, D. A., & McCormick, F. (1990) *Nature 348*, 125–132.
Bourne, H. R., Sanders, D. A., & McCormick, F. (1991) *Nature 349*, 117–127.
Calés, C., Hancock, J. F., Marshall, C. J., & Hall, A. (1988) *Nature 332*, 548–551.
Campbell-Burk, S. (1989) *Biochemistry 28*, 9478–9484.
Campbell-Burk, S., Papastavros, M. Z., McCormick, F., & Redfield, A. G. (1989) *Proc. Natl. Acad. Sci. U.S.A. 86*, 817–820.
Campbell-Burk, S. L., Domaille, P. J., Starovasnik, M. A., Boucher, W., & Laue, E. D. (1992) *J. Biomol. NMR 2*, 639–646.
Cen, H., Papageorge, A. G., Zippel, R., Lowy, D. L., & Zhang, K. (1992) *EMBO J. 11*, 4007–4015.
Clore, G. M., & Gronenborn, A. M. (1991) *Prog. NMR Spectrosc. 23*, 43–92.
Créchet, J. B., Poullet, P., Mistou, M. Y., Parmeggiani, A., Camonis, J., Boy-Marcotte, E., Damak, F., & Jacquet, M. (1990) *Science 248*, 866–868.
Downward, J. (1992) *BioEssays 14*, 177–184.
Feuerstein, J., Goody, R. S., & Webb, M. R. (1989) *J. Biol. Chem. 264*, 6188–6190.
Griffey, R. H., & Redfield, A. G. (1987) *Q. Rev. Biophys. 19*, 51–82.
Hall, A. (1990) *Science 249*, 635–640.
Hanahan, D. (1983) *J. Mol. Biol. 166*, 557–580.
Hata, Y., Kaibuchi, K., Kawamura, S., Hiroyoshi, M., Shirataki, H., & Takai, Y. (1991) *J. Biol. Chem. 266*, 6571–6577.
John, J., Sohmen, R., Feuerstein, J., Linke, R., Wittinghofer, A., & Goody, R. S. (1990) *Biochemistry 29*, 6058–6065.
Jurnak, F., Heffron, S., & Bergmann E. (1990) *Cell 60*, 525–528.
Latwesen, D. G., Poe, M., Leigh, J. S., & Reed, G. H. (1992) *Biochemistry 31*, 4946–4950.
LeMaster, D. M., & Richards, F. M. (1988) *Biochemistry 27*, 142–150.
Lowe, D. G., Ricketts, M., Levinson, A. D., & Goeddel, D. V. (1988) *Proc. Natl. Acad. Sci. U.S.A. 85*, 1015–1019.
Lowy, D. R., Zhang, K., DeClue, J. E., & Willumsen, B. M. (1991) *Trends Genet. 7*, 346–351.
Martegani, E., Vanoni, M. A. G., Zippel, R., Coccetti, P., Brambilla, R., Ferrari, C., Sturani, E., & Alberghina, L. (1992) *EMBO J. 11*, 2151–2157.
Martin, G. A., Yatani, A., Clark, R., Conroy, L., Polakis, P., Brown, A. M., & McCormick, F. (1992) *Science 255*, 192–194.
Masters, S. B., Sullivan, K. A., Miller, R. T., Beiderman, B., Lopez, N. G., Ramachandran, J., & Bourne, H. R. (1988) *Science 241*, 448–451.
Masters, S. B., Landis, C. A., & Bourne, H. R. (1990) *Adv. Enzyme Regul. 30*, 75–87.
McIntosh, L. P., Wand, A. J., Lowry, D. F., Redfield, A. G., & Dahlquist, F. W. (1990) *Biochemistry 29*, 6341–6362.
Milburn, M. V., Tong, L., deVos, A. M., Brünger, A., Yamaizumi, Z., Nishimura, S., & Kim, S.-H. (1990) *Science 247*, 939–945.
Miller, A.-F., Papastavros, M. Z., & Redfield, A. G. (1992) *Biochemistry 31*, 10208–10216.

Mistou, M. Y., Jacquet, E., Poullet, P., Rensland, H., Gideon, P., Schlichting, I., Wittinghofer, A., & Parmeggiani, A. (1992) *EMBO J. 11*, 2391–2397.

Mizuno, T., Kaibuchi, K., Yamamoto, T., Kawamura, S., Sakodo, T., Fujioka, H., Matsuura, Y., & Takai, Y. (1991) *Proc. Natl. Acad. Sci. U.S.A. 88*, 6442–6446.

Muchmore, D. C., McIntosh, L. P., Russell, C. B., Anderson, D. E., & Dahlquist, F. W. (1989) *Methods Enzymol. 177*, 44–73.

Muto, Y., Yamasaki, K., Ito, Y., Yajima, S., Masaki, Y., Uozumi, T., Walchli, M., Nishimura, S., Miyazawa, T., & Yokoyama, S. (1993) *J. Biomol. NMR 3*, 165–184.

Pai, E. F., Krengel, U., Petsko, G. A., Goody, R. S., Kabsch, W., & Wittinghofer, A. (1990) *EMBO J. 9*, 2351–2359.

Redfield, A. R., & Papastavros, M. Z. (1990) *Biochemistry 29*, 3509–3514.

Schaber, M. D., Garsky, V. M., Boylan, D., Hill, W. S., Scolnick, E. M., Marshall, M. S., Sigal, I. S., & Gibbs, J. B. (1989) *Proteins: Struct., Funct., Genet. 6*, 306–315.

Schlichting, I., Almo, S. C., Rapp, G., Wilson, K., Petratos, K., Lentfer, A., Wittinghofer, A., Kabsch, W., Pai, E. F., Petsko, G. A., & Goody, R. S. (1990) *Nature 345*, 309–315.

Shou, C., Farnsworth, C. L., Neel, B. G., & Feig, L. A. (1992) *Nature 358*, 351–358.

Szeberenyi, J., Cai, H., & Cooper, G. M. (1990) *Mol. Cell. Biol. 10*, 5324–5332..

Tong, L., de Vos, A. M., Milurn, M. V., & Kim, S.-H. (1991) *J. Mol. Biol. 217*, 503–516.

Trahey, M., & McCormick, F. (1987) *Science 238*, 542–545.

Valencia, A., Kjeldgaard, M., Pai, E. F., & Sander, C. (1991) *Proc. Natl. Acad. Sci. U.S.A. 88*, 5443–5447.

Verrotti, A. C., Créchet, J. B., Blasi, F. D., Seidita, G., Mirisola, M. G., Kavounis, C., Nastopoulos, V., Burderi, E., Vendittis, E. D., Parmeggiani, A., & Fasano, O. (1992) *EMBO J. 11*, 2855–2862.

Willumsen, B. M., Vass, W. C., Velu, T. J., Papageorge, A. G., Schiller, J. T., & Lowy, D. R. (1991) *Mol. Cell. Biol. 11*, 6026–6033.

Wittinghofer, A., & Pai, E. F. (1991) *Trends Biochem. Sci. 16*, 382–387.

Wolfman, A., & Macara, I. G. (1990) *Science 248*, 67–69.

Wüthrich, K. (1986) *NMR of Proteins and Nucleic Acids*, J. Wiley and Sons, New York.

Yamasaki, K., Kawai, G., Ito, Y., Muto, Y., Fujita, J., Miyazawa, T., Nishimura, S., & Yokoyama, S. (1989) *Biochem. Biophys. Res. Commun. 162*, 1054–1062.